Journal of Magnetism and Magnetic Materials 81 (1989) 29–38
North-Holland, Amsterdam

TAYLOR-VORTEX FLOW OF FERROFLUIDS IN THE PRESENCE OF GENERAL MAGNETIC FIELDS

M. NIKLAS, H. MÜLLER-KRUMBHAAR
Institut für Festkörperforschung, KFA Jülich, D-5170 Jülich, Fed. Rep. Germany

and

M. LÜCKE
Institut für Theoretische Physik, Universität des Saarlandes, D-6600 Saarbrücken, Fed. Rep. Germany

Received 29 March 1989

The influence of magnetic fields on the flow of a magnetic fluid in the gap between two concentric rotating cylinders is investigated by linear analysis and explicit finite-difference numerical solution of the full nonlinear time-dependent field equations. An oscillatory instability of the primary flow towards Taylor vortices predicted by Vislovich et al. (1986) on the basis of a linear analysis for a superposition of axial and radial magnetic fields is confirmed. Detailed investigations show further that this instability manifests itself as a travelling pattern which can be found also in a finite system. In a wide region in parameter space nonaxisymmetric flow patterns appear as the primary instability. An axial-azimuthal magnetic field generates an axial flow, sustaining a net mass transport in axial direction.

1. Introduction

Ferrofluids or magnetic fluids are suspensions of small (Ø ≈ 10 nm) magnetic particles. Compared to ordinary liquids they exhibit a wealth of new phenomena when magnetic fields are applied [1]. This is already exploited in many technical applications [2] and has stimulated basic research (e.g. see ref. [3]).

Here we investigate the effect of general magnetic fields on the flow of a magnetic fluid in the gap between two concentric cylinders of which the inner one is rotating. There for ordinary fluids the primary, purely azimuthal Couette flow is unstable against axially periodic Taylor vortices if the rotation velocity Ω_1 of the inner cylinder of radius R_1 (outer cylinder of radius R_2 is a rest) exceeds a critical value $\Omega_{1,c}$. To parametrize the driving we either use the Taylor number

$$T = 2\left(\frac{R_1\Omega_1 d}{\nu}\right)^2\left(\frac{1-\eta}{1+\eta}\right). \qquad (1)$$

or

$$\epsilon' = \frac{\Omega_1}{\omega_{1,c}} - 1 \qquad (2)$$

which measures the reduced deviation of the rotation rate from the critical one. Here $d = R_2 - R_1$, $\eta = R_1/R_2$ and ν denotes the kinematic viscosity. The periodic pattern appears at threshold with a unique wave number k_c (for reviews see refs. [4–6]).

For magnetic fluids Berkovsky et al. [7] determined in 1984 the stabilizing effect of an axially oriented magnetic field on the primary, purely azimuthal Couette flow. Their results have been confirmed by independent investigations [8,9] which beyond that considered also the effect of radially and azimuthally oriented (≙ simple) magnetic fields on the critical parameters Taylor number T_c and wave number k_c of the periodic Taylor vortex pattern in a 'narrow gap' $\eta \approx 1$. In this limit Vislovich et al. [10] investigated by linear

0304-8853/89/$03.50

stability analysis the stability of Couette flow towards axisymmetric Taylor vortices in a more general magnetic field: in a superposition of radial and axial magnetic fields they found an oscillatory instability which could give rise either to a travelling Taylor vortex pattern or a standing one in the finite cylinders assumed. Here we extent their linear investigations to a full nonlinear evaluation of the flow field. Therein we always found the travelling vortex pattern to be realized, i.e. to be the stable one. Further on we determine the influence of the end plates of a finite cylinder on the travelling vortex pattern. For nonaxisymmetric disturbances of the primary Couette-flow we show in a linear analysis that in radial-axial magnetic fields, infinite cylinders and a 'narrow gap' these disturbances appear as primary instability instead of the axisymmetric Taylor vortices for a wide region in parameter space. Finally, we elucidate some interesting phenomena in a superposition of axially and azimuthally oriented magnetic fields.

The results presented below are obtained by linear stability analysis and explicit finite difference numerical solution of the full nonlinear time-dependent field equations of motion. The double characteristic eigenvalue problem one arrives at in the linear stability analysis when overstability is taken into account has been solved with high precision [11] using a shooting method [12] and a modified Newton–Raphson-method [13]. The finite difference numerical solution is based on the staggered MAC-grid [14] using the SMAC-method [15]. A homogeneous grid spacing of $d/20$ has been found small enough to produce results of sufficient accuracy. Further details on the numerics are given in refs. [8,11]. The relative high accuracy and satisfactory overall performance of this grid scheme has been demonstrated in a recent comparison [16] of nine different finite-difference schemes.

2. Basic equations

The magnetic fluid is assumed to be incompressible, nonconducting, to have a constant temperature and a homogeneous distribution of the small magnetic particles within the suspension. Starting from general conservations laws [1] and using the equation of relaxation for magnetization derived phenomenologically by Shliomis [17,18] one arrives [8,11] at the field equations of motion for magnetic fluids which are valid for timescales large compared to the Brownian time of relaxation being of the order of 10^{-6} s for magnetic fluids [18]:

$$\begin{aligned}\rho\frac{\mathrm{d}}{\mathrm{d}t}\boldsymbol{v} = & -\nabla p + \tilde{\eta}\nabla^2\boldsymbol{v} + c'(H) \\ & \times\{(\boldsymbol{H}\times[\boldsymbol{\Omega}\times\boldsymbol{H}])\times\nabla|\boldsymbol{H}|\} \\ & + c(H)\{\nabla\times(\boldsymbol{H}\times[\boldsymbol{H}\times\boldsymbol{\Omega}]) \\ & - 2([\boldsymbol{H}\times\boldsymbol{\Omega}]\cdot\nabla)\boldsymbol{H}\}. \qquad (3a)\end{aligned}$$

This may be written in a sometimes more useful form (with $\boldsymbol{F} = \mathrm{rot}\ \boldsymbol{v}\times\boldsymbol{H} = \boldsymbol{\Omega}\times\boldsymbol{H}$)

$$\begin{aligned}\rho\frac{\mathrm{d}}{\mathrm{d}t}\boldsymbol{v} = & -\nabla p + \tilde{\eta}\nabla^2\boldsymbol{v} + c'(H) \\ & \times\{(\boldsymbol{H}\times\boldsymbol{F})\times\nabla|\boldsymbol{H}|\} \\ & + c(H)\{\boldsymbol{F}\nabla\cdot\boldsymbol{H} - \boldsymbol{H}\times(\nabla\times\boldsymbol{F}) \\ & - \boldsymbol{H}\nabla\cdot\boldsymbol{F}\}. \qquad (3b)\end{aligned}$$

Here $\boldsymbol{v} = (u, v, w)$ denotes the velocity of the magnetic fluid, $\boldsymbol{\Omega} = \nabla\times\boldsymbol{v} = \mathrm{rot}\ \boldsymbol{v}$ its vorticity, $\mathrm{d}\circ/\mathrm{d}t = \partial\circ/\partial t + (\boldsymbol{v}\cdot\nabla)\circ$, $\boldsymbol{H}$ the magnetic field, $c(H) \equiv \frac{1}{4}\tau_\perp\mu_0 M_0/H$ and $c'(H)$ its derivative with respect to $H = |\boldsymbol{H}|$, M_0 the equilibrium magnetization, μ_0 the permeability and $\tau_\perp(H)$ the relaxation time constant for the component of the magnetization orthogonal to the magnetic field. Following Shliomis [18] one can interpret $c(H)H^2$ as additional rotational viscosity $\tilde{\eta}_r$. $\tilde{\eta}_r$ reflects the fact that the free rotation of the magnetic particles due to the local vorticity $\boldsymbol{\Omega}$ of the fluid is hindered by the magnetic volume force which tends to align the magnetic moments being fixed to the particle parallel to the magnetic field. Obviously this hindrance does not appear if $\boldsymbol{\Omega}$ and $\boldsymbol{H}$ are parallel. Eqs. (3) shows this anisotropy of the rotational viscosity since all additional terms are proportional to $\boldsymbol{F} = \boldsymbol{\Omega}\times\boldsymbol{H}$. All information of the specific properties of the magnetic fluid (e.g. concentration, specific materials) and the strength of the magnetic field are collected in $\tilde{\eta}_r$ which is conveniently given in units of viscosity $\tilde{\eta} = \nu\rho$ in the absence of a magnetic field

$$S = \frac{c(H)H^2}{\tilde{\eta}} = \frac{\tilde{\eta}_r}{\tilde{\eta}} = \frac{\nu_r}{\nu}. \quad (4)$$

No-slip boundary conditions have been imposed on the velocity field at the inner (outer) cylinder of radius R_1 (R_2) rotating at velocity $V_1 = \Omega_1 R_1$ (0). When considering infinite systems, periodic boundary conditions are assumed in axial direction with various periodicity lengths specified in the text. In a finite system of length $L = \Gamma d$ the end plates are assumed to be attached to the stationary outer cylinder and enforce no-slip conditions.

3. Superposition of radial and axial magnetic fields

In this section we limit ourselves to the approximation of a 'narrow gap' since it is very difficult to realize radial magnetic fields experimentally in a wide gap. Thus we take $\eta \to 1$ in the linear stability analysis and $\eta = 0.95$ in the numerical simulation. Then the magnetic field $\boldsymbol{H} = (H_r/r)\boldsymbol{e}_r + H_z\boldsymbol{e}_z$ can be considered constant in magnitude across the gap width d (terms $\approx \nabla|\boldsymbol{H}|$ drop in eq. (3)) and characterized by its magnitude H and the angle $\alpha = \arctan(H_r/R_1H_z)$ between its orientation and the z-axis. For a detailed investigation the equation of motion (3) is specialized for this superposition of radial and axial magnetic fields and S and α are used as tuning parameters for the system. From the equations obtained (they are explicitly given in ref. [11]) one can see that in an infinite cylinder gap the primary flow is the circular Couette flow already known from ordinary liquids.

3.1. Infinite system

3.1.1. Linear stability against axisymmetric disturbances

Assuming axisymmetry one can determine the stability of this flow by the ansatz that the perturbation of the primary Couette flow are $\approx \exp\{ikz + \sigma t + i\omega t\}$. Then from linear stability analysis one obtains the critical Taylor number T_c and the critical wave number k_c which are 1694.950195 and 3.12657, respectively, for normal fluids. For magnetic fluids these two critical parameters are shown in fig. 1 as a function of the angle α between the orientation of the magnetic field and the z-axis for $S = 1$. Also given are the results of Vislovich et al. [10] (dashed lines). A comparison shows a quite good qualitative agreement: by changing S from 0 to 1 the critical Taylor number is increased by about a factor of three and by varying α the size of the periodic vortices can be modified. Quantitatively, however, there are slight differences: the high precision results of the present investigation show an influence of α on the critical Taylor number which is symmetric about 90° as it should be. The deviations of the critical wave number may be explained by the inaccuracy of about 3% in the determination of the critical Taylor number which has a strong influence on k_c [12].

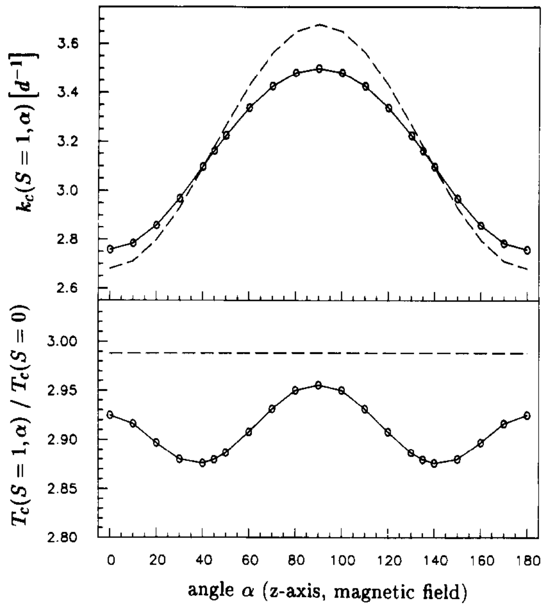

Fig. 1. The critical wave number k_c and the reduced critical Taylor number T_c vary with the orientation of the magnetic field ($S = 1$). Dashed lines are results of ref. [10].

In contrast to normal fluids magnetic fluids exhibit an oscillatory instability towards Taylor vortices, that is, ω has a finite nonzero value ω_c at the marginal curve where σ changes sign [6]. This

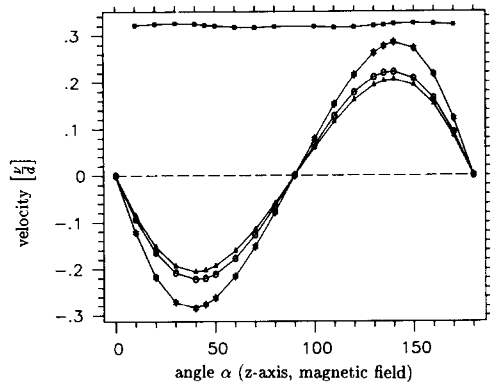

Fig. 2. Group velocity (*) and phase velocity (▲) resulting from the linear analysis vary with the orientation of the magnetic field ($S=1$). The (phase) velocities of the Taylor vortex pattern observed in a numerical simulation ($\epsilon' = 0.04$, ∘) are a little bit larger, the ratio however (■ = (▲/∘)0.35) is nearly constant. The vortex pattern always moves opposite to the z-component of the magnetic field.

result of Vislovich et al. is confirmed by the present investigation. The results for the phase velocity $v_{\mathrm{ph}} = \omega_c/k_c$ and the group velocity $\partial w_c/\partial k|_{k_c,T_c}$ are given in fig. 2 by the '▲' and the 'stars', respectively ($S=1$). One clearly sees that both velocities have a definite sign: they are always directed opposite to the z-component of the applied magnetic field. This breaking of the mirror symmetry in the Taylor Couette system is caused by the applied magnetic field. For $0° < \alpha < 90°$ the magnetic field lines move upward with increasing radial coordinate while for $90° < \alpha < 180°$ they move opposite to the z-axis. The orientational dependence of the group velocity on α in magnetic fluids has recently been used to confirm the linear influence of the group velocity on the propagation velocity of a propagating front as predicted by an amplitude equation [19].

3.1.2. Numerical solution of the full axisymmetric field equations

The values for the phase velocities may be compared with the results of the finite-difference numerical solution of the time dependent field equations. Using periodic boundary conditions in axial direction the corresponding Hopf-bifurcating solution has always been found as an axially travelling Taylor vortex pattern with a constant phase velocity. Similar to convection in binary mixtures a standing wave seems to be unstable in favour of a travelling one. Values for the propagation velocity are given in fig. 2 by the open circles ∘, the parameters choosen there are $S=1$, $\eta = 0.95$ and $\Omega_1 = 1.04\Omega_{1,c}$. The α-dependence is the same as given already in linear stability. The values of the linear stability analysis are about 8% smaller than those actually observed in numerical simulation. This small discrepancy can be partially understood as being caused by a dependence of the phase velocity on the distance, $\epsilon' = 0.04$, to the critical point. The remaining part, about 4%, can be attributed to differences in the method of investigation and the idealizing approximation 'narrow gap' used in the linear stability analysis. However, the ratio ■ = (▲/∘)0.35 of both phase velocities is nearly constant (fig. 2), thus the result, especially the α-dependence, corroborate each other. All our results indicate that the Hopf-bifurcation of the basic Couette flow to the travelling Taylor vortex pattern is a forward one as the stationary bifurcation without magnetic field.

A snapshot of the travelling Taylor vortex pattern in the axially periodic gap is given in fig. 3: Shown are isolines of the streamfunction Ψ defined by $w = (1/r)\partial_r\Psi$ and $u = (1/r)\partial_z\Psi$ which were determined from the velocity field by solving a Poisson-equation with the very efficient 'conjugate-gradient-method' [20]. The inner (outer) cylinder is left (right), the parameters chosen are $\eta = 0.95$, $S=1$, $\Omega_1 = 1.02\Omega_{1,c}$, $\alpha = 45°$ and an axial periodicity length of $1.991d$. Full (dashed)

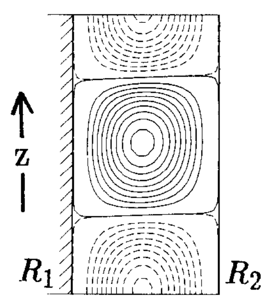

Fig. 3. Isoline patterns of the streamfunction $\Psi(ru \equiv -\partial_z\Psi, rw \equiv \partial_r\Psi)$ in the gap with axial periodicity length $1.991d$. $\eta = 0.95$, $\alpha = 45°$, $S=1$, $\epsilon' = 0.02$. The pattern travels downwards in negative z-direction.

lines mark clockwise (counterclockwise) rotating vortices. Both kinds of vortices are similar, apart from their orientation of rotation. The line separating the two vortices is straight but not orthogonal to the cylinder walls. It deviates from this direction by about 2°. Such an oblique separating line has been observed also by Vislovich et al. [10] in their linear analysis. From their fig. 2 one may deduce an angle of about 17°. The difference may be attributed to different parameters. We have chosen with the periodicity length $1.991d$ the critical wavelength while they used a value of $k = 2.5$ which is to our opinion not necessarily Eckhaus stable. Furthermore their rotation velocity of the inner cylinder is larger. At $\alpha = 45°$ the pattern travels downwards. It has been checked whether this axial pattern propagation is accompanied by some mean axial flow such that there is a net axial fluid flow. Within the accuracy of the numerics this is not the case. Thus travelling Taylor vortices in a radial-axial magnetic field show some analogy to acoustic waves and small amplitude surface waves.

3.1.3. Linear stability against nonaxisymmetric disturbances

In the classical Taylor-Couette-system for normal fluids and independently rotating cylinders there are regions in parameterspace where non-axisymmetric disturbances in e.g. spiral form apear as primary instability of the primary Couette flow [4,5]. Even if the outer cylinder is at rest non-axisymmetric disturbances appear only slightly above the critical rotation rate of the inner cylinder (e.g. about 5% for a radius ratio $\eta = 0.95$ (ref. [4], and refs. therein)). Hence it is worthwhile to investigate whether this sequence is reversed in magnetic fluids if radial-axial magnetic fields are applied.

The derivatives with respect to the azimuthal coordinate which have been neglected so far in the equation of motion have to be considered now. The primary flow is still the Couette flow. Non-axisymmetric disturbances to this flow are of the kind $\sim \exp\{\sigma t + \mathrm{i}(\omega t + kz + m\varphi)\}$. For the flow field to be defined in a unique way m has to be an integer. The perturbation velocity field now depends on two variables, the radial coordinate and $(\omega t + kz + m\varphi)$. For $m \neq 0$ there are non-axisymmetric disturbances under investigation, e.g. for $m = 1$ a helicoidal pattern similar to a barbers pole.

Considering $m \neq 0$ it is impossible within the framework of a linear stability analysis to distinguish between a flow pattern travelling in azimuthal direction and representing a standing wave in axial direction and a second one which is travelling in both axial and azimuthal direction [21]. To clarify this point the whole nonlinear equations would have to be considered. Within linear stability it is only possible to state if non-axisymmetric disturbances show up at a Taylor number smaller than that for axisymmetric ones. And this is the question that we have investigated.

Having regard to the derivatives with respect to the azimuthal coordinate, we specialize again on the narrow gap approximation. As pointed out by Krueger et al. [21], the variable φ has to be scaled in a convenient and straightforward way within the narrow gap approximation at which one arrives automatically if all curvature effects are treated in the same way as the centrifugal term in the normal fluid Taylor–Couette-system. For the interpretation of the results we chose, following Krueger et al., a value of $\eta = (1/(1 + \delta)$ with $\delta = 1/20$ which is considered to be sufficiently small to allow comparison to experiments in a narrow gap. The double characteristic eigenvalue problem resulting for $T(k, m, S, \alpha)$ and $\omega(k, m, S, \alpha)$ has been solved for $m = 0, \ldots, 5$. By comparison one can determine for a pair (S, α) that mode m towards which the primary Couette flow is unstable first: it is the one with the minimal Taylor number. As fig. 4 shows, both axisymmetric ($m = 0$) and non-axisymmetric ($m \neq 0$) modes are possible as primary instability depending on S and α. The points mark the combinations (S, α) in parameter space where investigations have been performed and $m = 0$ modes (■), $m = 1$ (●) and $m = 2$ modes (▲) have been found as primary disturbances. The separating lines are guides to the eye. The parameter S has been enlarged above the value of 1 (which is considered as an upper limit for real magnetic fluids) to demonstrate the structure of the phase diagram more clearly – at even larger values of S even larger values of m appear at

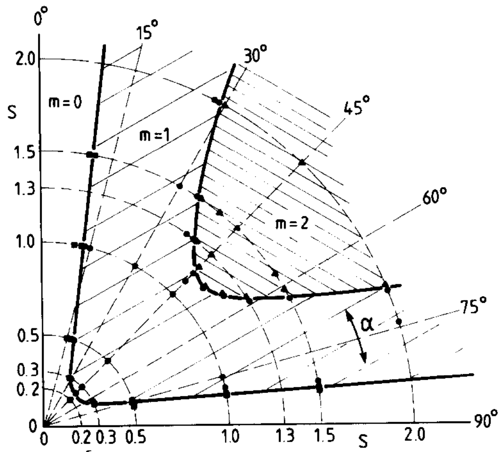

Fig. 4. Instability diagram of Couette flow. Nonaxisymmetric disturbances ($m \neq 0$) appear in a wide region of the parameter space (α, S) as the primary instability. See text for more details.

$\alpha = 45°$. The phase diagram is not strictly symmetric about $\alpha = 45°$ but the regions are tilted slightly to larger α's. Fig. 4 stresses that nonaxisymmetric disturbances play an important role especially at larger S-values. However, one cannot say within linear stability analysis how this makes itself felt in developed flow patterns. This has to be clarified in an analysis of the whole nonlinear and nonaxisymmetric equations of motion.

3.2. Finite system

So far we have considered a cylinder gap extended infinitely in axial direction. End plates always present in real experiments modify the flow behaviour drastically. In a normal fluid the vanishing of the azimuthal flow component at the end plates cause vortex flow near the ends which is present even in the subcritical region [22], see also fig. 5 left. For $T < T_c$ the amplitude of the vortices decays exponentially with increasing distance from the end plates. Yet for $T \to T_c$ this exponential decay length diverges and these Ekman-vortices extend throughout the whole cylinder gap [22].

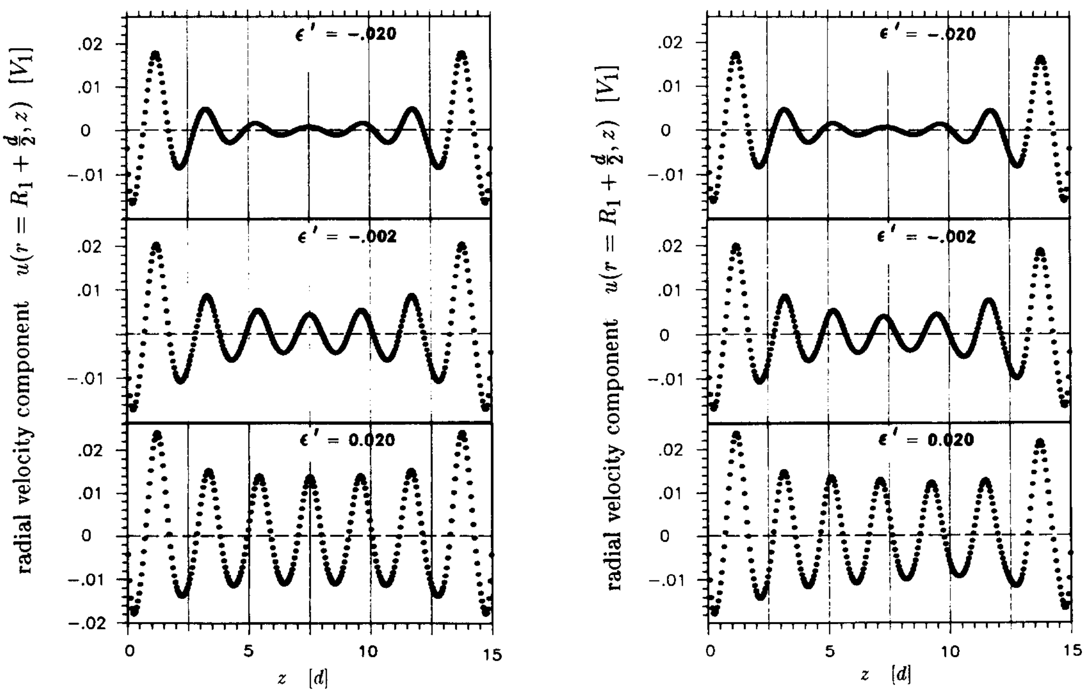

Fig. 5. Radial velocity component u in the middle of the gap for different drivings. $\Gamma = 15$, $\eta = 0.95$. The midplane symmetry presents in normal fluids (left) is no longer given in magnetic fluids in a radial-axial magnetid field with $S = 0.2$, $\alpha = 45°$ (right).

In this section we investigate the effects of a finite length on the flow of a magnetic fluid in radial-axial magnetic fields. Of special interest is whether these axisymmetric Ekman-vortices at the boundaries cause a 'pinning' of the travelling Taylor vortex pattern observed in infinite cylinders. At present numerical simulation seems to be the theoretical method suited best to study the possibly time-dependent flow properties in the nonlinear region where vortex flow has a finite amplitude (especially that near the end plates). Here we again use explicit finite difference numerical simulation under the assumption of axisymmetry.

From the continuous range of angles between the radial-axial magnetic field and the z-axis we specialize for the investigation on $\alpha = 45°$ as a characteristic representative. Numerical simulation for $S = 0.2$, $\eta = 0.95$ and an axial length $\Gamma = L/d = 15$ shows (fig. 5) that even at subcritical values of the driving the magnetic field makes itself felt in the magnetic fluid. The minimum of the vortex flow amplitude which is located at the midheight ($z = 7.5d$) in normal fluids is no longer at that place. The vortices in the middle or 'bulk' of the gap are shifted downwards to smaller z-values by about a quarter of vortex diameter. The direction opposite to the z-component of the magnetic field agrees with the results for the travelling pattern in the infinite gap. Yet for the parameters specified one obtains stationary states.

If one increases however, the driving of the inner cylinder to $\epsilon' = 0.04$ and considers $S = 1$, time periodic states appear in the bulk of the system. What happens can be seen best in fig. 6. In the middle of the gap the vortices are travelling downwards. They appear in the top part and vanish in the bottom part. A 'pinning' of this travelling pattern by the Ekman-vortices near the end plates does not occur. Nevertheless a finite gap length does have a distinct influence. Investigations with a different Γ but otherwise identical parameters show that travelling vortices appear only above a threshold value of $\Gamma = 11$. At smaller values one finds stationary, asymmetric flow states with vortices shifted downwards as described above. And with increasing Γ the traveling velocity of the travelling vortices in the middle of the gap approaches the value of the infinite cylinder as it should be. The latter value has been determined separately by applying periodic boundary

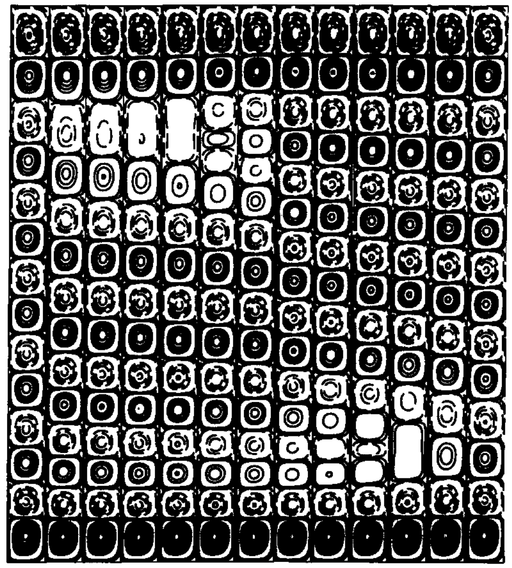

Fig. 6. Snapshots of the streamfunction Ψ at 13 successive times. In a finite gap bounded by endplates an additional vortex pair is periodically created close to the top. Vortices in the middle move from up to bottom where another vortex pair disappears periodically. The period is $10.075\,[d^2/\nu]$ for $\epsilon' = 0.04$, $\Gamma = 15$, $\eta = 0.95$, $S = 1$, $\alpha = 45°$. The inner (outer) cylinder is always left (right). Full (dashed) lines mark clockwise (counterclockwise) rotating vortices.

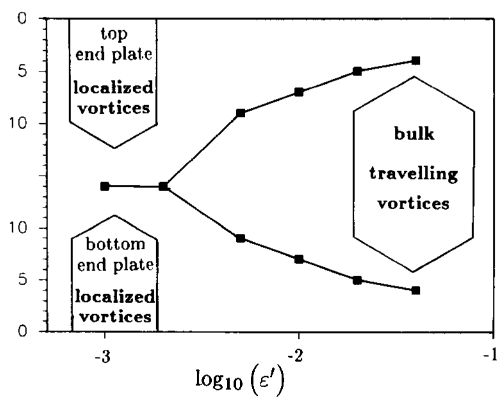

Fig. 7. Number of the last vortex counted from the corresponding end plate that does not move (cf. fig. 6). In between travelling vortices exist. Symbols connected by full lines mark stationary states ($S = 0.2$, $\alpha = 45°$). The influence of the end plates on the flow within the whole gap increases with decreasing driving ϵ'.

conditions in axial direction. A finite length of the gap reduces the velocity slightly until the travelling stops abruptly when Γ reaches the threshold value 11.

It was mentioned already that the extension of the Ekman vortex system diverges as $\epsilon' \to 0$. Thus with $\epsilon' \to 0$ the influence of the localized vortices near the end plates on the flow field in the entire gap increases. Fig. 7 demonstrates that this is also valid for magnetic fluids in a radial-axial magnetic field. To larger values of the driving ϵ' the region of travelling vortices, the 'bulk'-region, is strongly extended. With decreasing driving the number of vortices which stay immobile and localized near the end plates increases monotonously. The influence of the end plates is for $\epsilon' < 0.002$ so strong that one observes after some oscillations only a stationary asymmetric flow pattern.

This system exhibits some interesting similarities to convection in binary mixtures. In a finite container Walden et al. [23] observed 1985 in a water–ethanol-mixture travelling waves. This has been confirmed in recent experiments and numerical simulations, a 'pinning' is not obsereved. However there is a difference: in contrast to the Taylor–Couette-system there are no permanent vortices near the boundaries in Rayleigh–Bénard-systems. That is why the vortices appear directly near the side walls of the container.

Finally, we want to stress again that the numerical simulation is based on the assumption of axial symmetry. The results of the previous section point out that this is not always justified. Nevertheless, the main statement 'there exist travelling waves in a finite cylinder' continues to be valid. The reason is that e.g. for spiral shaped $m = 1$ modes a (rotating) point defect is sufficient to produce a pattern travelling in axial direction while for the axisymmetric modes considered here a line defect is necessary. The latter is a more stringent restriction. Therefore, one can expect nonaxisymmetric vortices to travel if the axisymmetric do so.

4. Superposition of axial and azimuthal magnetic fields

In this section we consider the flow in a superposition of axial and azimuthal magnetic fields: $\boldsymbol{H} = (H_\phi/r)\boldsymbol{e}_\phi + H_z\boldsymbol{e}_z$. For a wide gap (we specialize on $\eta = 0.5$) the radial dependence of the azimuthal component cannot be neglected. Thus, in a description of the magnetic field by its magnitude H and its orientation by the angle β with respect to $\boldsymbol{e}_\varphi$ one has to consider that both quantities depend on the radial coordinate. For simplicity the following situation is investigated only: a strong magnetic field where H_φ and H_z are adjusted in such a way that the angle β_0 has a value of 45° at the inner cylinder. Thus $\beta(r) = \arctan\{(r/R_1)\tan\beta_0\}$. Furthermore $\nabla|\boldsymbol{H}| = -H\cos^2\beta(1/r)\boldsymbol{e}_r$ and $c'(H) = \partial_c(H)/\partial H$ may be expressed as $-2c(H)/H$ since the rotational viscosity $\tilde{\eta}_r(H) = c(H)H^2$ saturates in strong magnetic fields resulting in $\partial\tilde{\eta}_r/\partial H \to 0$.

The field equations of motion one finally arrives at when specializing eqs. (3) for this field have been investigated for $S = 1$ and $\beta_0 = 45°$ by the finite-difference code assuming axisymmetry. Considering an infinite cylinder gap (periodic boundary conditions in axial direction) it turns out that the stationary primary flow is not identical to the Couette flow. The azimuthal component deviates in a very small way from the classical Couette profile, its curvature is a little bit larger than the classical one. More important is the fact that the primary flow shows a nonvanishing axial component w of a nearly parabolic shape with a magnitude which is less than 1% of the maximal azimuthal velocity component. We have reproduced and checked this result of the full nonlinear simulation code by a special computation of the primary flow [11] using the fact that it has no radial component and that it does not depend on the axial coordinate z. The occurrence of a modified primary flow is somehow surprising although one has found in viscoelastics in the Taylor-system that the purely axisymmetric primary Couette flow does not represent a solution for all values of the control parameter [24].

While increasing the rotation rate of the inner cylinder here again Taylor vortices appear. The critical parameters have been determined by the finite-difference code from the relaxational behaviour of the flow for $S = 1$ to be $T_c = 7614.13$ and $k_c = 2.88$. An arrow plot of the flow field components u and w slightly above the critical

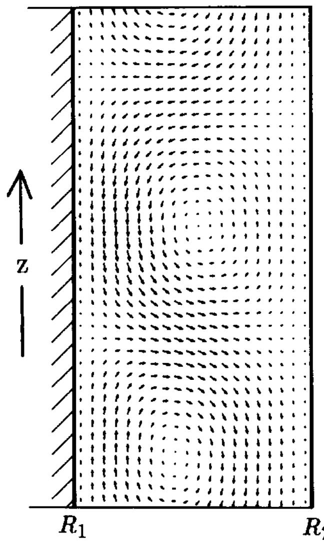

Fig. 8. Flow field of magnetic fluids in an axial-azimuthal magnetic field ($S=1$, $\epsilon'=0.02$, $\eta=0.5$, axial periodicity lenghs $2.18d$, $\beta_0=45°$).

value ($\Omega_1 = 1.02\Omega_{1,c}$) is given in fig. 8. Taylor vortices are superposed on a primary flow pointing downwards. The centers of the vortices are shifted relative to each other. If one increases the rotation rate of the inner cylinder further the asymmetric situation with respec to the radial coordinate is reversed and the clockwise rotating vortex is enlarged at the cost of the counterclockwise one.

The variation of the net axial mean flow as a function of ϵ' has been investigated in more detail and the results are presented in fig. 9. For subcritical values of the driving i.e. in the absence of vortices there exists a net flow in the direction opposite to the z-component of the magnetic field which is due to the nonvanishing axial component of the primary flow. This integral value is independent of the driving ϵ'. (The driving drops out of the equations for the primary flow – $u=0$, $v=v(r)$, $w=w(r)$ – if the velocities are scaled in units of $|V_1|$. Thus, the unreduced velocity field of the primary flow varies linearly with the velocity of the inner cylinder.) The Taylor vortices that are present above threshold, $\epsilon'>0$, in this magnetic field are such that they generate an additional mean flow. However, the vortex generated mean flow grows with ϵ' and, furthermore, is directed opposite to constant primary flow. The net flow being the sum of these two contributions changes sign at $\epsilon'=0.18$ for the parameters of fig. 9. To larger values of the driving there exists a net flow in the direction of the axial magnetic field component, also the Taylor vortices travel in this direction. All these directions are reversed by a change in sign of β_0, as it should be.

Flows of the kind described above with a net mass flow in axial direction are not possible in a finite cylinder; due to incompressibility of the magnetic fluid the integrated axial flow has to vanish for any axial coordinate z. However, our simulation for finite cylinders shows that there is a circulating axial flow which is directed downward near the inner cylinder and which is balanced by a counterflow near the outer cylinder. Also for this magnetic field we observe for larger values of the driving travelling vortices in finite cylinders. Again a change in the sign of the magnetic field z-component is equivalent to a reflection of the flow field at the $z=\Gamma/2$ plane. One might wonder whether the axial-azimuthal magnetic field in its spiral form promotes nonaxisymmetric e.g. spiral shaped flows. This has to be clarified in a further investigation allowing also for nonaxisymmetric developed flows in the numerical simulation.

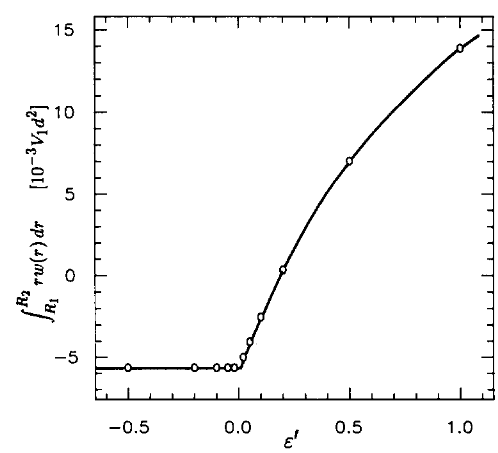

Fig. 9. Net mass flow through the gap as a function of the driving ϵ'. $S=1$, $\eta=0.5$, $\beta_0=45°$, periodicity lengths $2.18d$.

5. Conclusions

Summarizing we investigated within a model for the flow behaviour of magnetic fluids the effects of general magnetic fields on the flow between concentric rotating cylinders. Results of previous investigations have been confirmed, extended and quantitatively improved. Several new predictions are given. The various effects should stimulate experiments in this field.

References

[1] R.E. Rosensweig, Ferrohydrodynamics (Cambridge Univ. Press, Cambridge, 1985).
[2] R.E. Rosensweig, Advan. Electron. Electron Phys. 48 (1979) 103.
[3] Conf. Proc. IVth Intern. Conf. on Magnetic Fluids (1986), published in: J. Magn. Magn. Mat. 35 (2 & 3) (1987).
[4] R.C. DiPrima and H.L. Swinney, in: Hydrodynamic Instabilities and the Transition to Turbulence, eds. H.L. Swinney and J.P. Gollub (Springer, Berlin) Topics Appl. Phys. 45 (1981) 139.
[5] C.D. Andereck, S.S. Liu and H.L. Swinney, J. Fluid Mech. 164 (1986) 155.
[6] S. Chandrasekhar, Hydrodynamics and Hydromagnetic Stability (Oxford Univ. Press, Oxford, 1961).
[7] B.M. Berkovsky, V.Yu. Veretnov and S.M. Malyavin, 11th Riga Conf. on Magnetohydrodynamics, Riga, Latvian SSR, 1984, vol. 3 (Institut Fiziki AN Latviiskoi SSR, Riga, USSR, 1984) p. 115, in Russian.
[8] M. Niklas, Z. Phys. B 68 (1987) 493.
[9] M. Niklas, Poster at the IVth Intern. Conf. on Magnetic Fluids, Tokyo and Sendai, Japan (1986).
[10] A.N. Vislovich, V.A. Novikov and A.K. Sinitsyn, J. Appl. Mech. Tech. Phys. 27 (1986) 72.
[11] M. Niklas, Report of the Kernforschungsanlage Jülich GmbH Jül-2246 (December 1988).
[12] M.A. Dominguez-Lerma, G. Ahlers and D.S. Cannell, Phys. Fluids 27 (1984) 856.
[13] W.H. Press, B.P. Flannery, S.A. Teukolsky and W.T. Vetterling, Numerical Recipes – The Art of Scientific Computing (Cambridge Univ. Press, Cambridge, 1987).
[14] J.E. Welch, F.H. Harlow, J.P. Shannon and B.J. Daly, Los Alamos Scientific Laboratory Report, LA-3425 (1966).
[15] A.A. Amsden and F.H. Harlow, Los Alamos Scientific Laboratory Report, LA-4370 (1970).
[16] T.M. Shih, C.H. Tan and B.C. Hwang, Intern. J. Num. Meth. Fluids 9 (1989) 193.
[17] M.L. Shliomis, Sov. Phys. JETP 34 (1972) 1291.
[18] M.I. Shliomis, Sov. Phys. Usp. 17 (1974) 153.
[19] M. Niklas, M. Lücke and H. Müller-Krumbhaar, Europhys. Lett. (submitted).
[20] J. Stoer and R. Burlisch, Einführung in die Numerische Mathematik (Springer, Berlin, 1978).
[21] E.R. Krueger, A. Gross and R.C. DiPrima, J. Fluid Mech. 24 (1966) 521.
[22] G. Ahlers, D.S. Cannell, M.A. Dominguez-Lerma and R. Heinrichs, Physica D 23 (1988) 202.
[23] R.W. Walden, P. Kolodner, A. Passner and C.M. Surko, Phys. Rev. Lett. 55 (1985) 496.
[24] B.J.A. Zielinska and Y. Demay, Phys. Rev. A 38 (1988) 897.